CALORIMETRY OF THE Pd-D_2O SYSTEM: THE DRIVE TOWARDS HIGH LEVELS OF LOW GRADE HEAT

M. FLEISCHMANN* and S. PONS

IMRA Europe S.A.,

Science Center,

220 Rue Albert Caquot,

Sophia Antipolis,

06560 Valbonne,

France.

* to whom correspondence should be addressed

We outline some of the considerations which have prompted our search for anomalously fast nuclear reactions of D+ compressed electrochemically into Pd (and Pd-alloy) host lattices. The most surprising result has been that the generation of high levels of excess enthalpy is not accompanied by the expected levels of tritium and of neutron generation. We outline some of the major steps in the development of this particular aspect: it has been found that excess heat production is dependent on the protocol of the experiments mainly because of "positive feedback". A rationale for such "positive feedback" is presented which also explains oscillations in the system properties. We illustrate the progressive development leading up to the achievement of specific rates of excess enthalpy production of $\cong 4 kW cm^{-3}$ at temperatures up to $\cong 100°C$ (i.e. of low-grade heat).

Introduction

We have described elsewhere (see especially [1],[2],[3]) some of the reasons which led us to search for anomalously fast nuclear reactions of D^+ compressed eletrochemically into Pd and Pd-alloy host lattices. Of special importance was our knowledge of the key study by Coehn of the electrodiffusion of H^+ in fine wires of Pd [4]: one can conclude from this study that the mobility of H^+ in the lattice follows the Nerust-Einstein relation

$$u_{H^+} \cong \frac{F}{RT} D_{H^+} \tag{1}$$

so that the hydrogen is indeed present as protons* [2],[3]. The importance of this observation lies in the fact that an application of a Born-Haber cycle then shows that the protons sit in extremely deep energy wells, of the order $12eV/H^+$ [2],[3]. Such a conclusion would not in itself be remarkable were it not for the fact that we also know that the protons (or deuterons) are highly mobile: at sufficiently high charging ratios (H/Pd or D/Pd) they behave as classical oscillators, i.e. they are unbound in the lattice [7]. We can only resolve the conundrum of very tightly-bound yet highly mobile protons (or

* As we have noted elsewhere [3], this study dropped from view in the subsequent literature but reappeared following the investigation of Wagner and Heller [5]; a summary of numerous investigations up to 1978 is contained in [6]. These investigations have led to the rather strange conclusion that the protons are partially screened and the reported partial charges of the species are widely variable. However, as we have also noted [3], the experiment design of Coehn [4] was sound, whereas that of Wagner and Heller [5] was not; later experiments [6] have been based on the design of Wagner and Heller and this probably explains the fractional and widely varying charges on the proton which have been reported. Fractional charges can only arise if the given species is part of a larger quantum system (e.g. compare dipole moments). However, the argument which we develop in the main text is not critically dependent on the magnitude of the charge: the protons (or deuterons) must be deemed to be in deep energy wells even if they carry a fractional charge.

deuterons) by assuming that they are part of an extended (macroscopic) quantum system so that they can be intensely anharmonically excited. This dense proton or deuteron plasma (≅100M) coexists with an even more dense electron plasma (≅1000M) without formation of hydrogen or deuterium atoms and we probably need to invoke the intervention of a "third actor".

The fact that hydrogen and deuterium exist in the host lattice as protons and deuterons is also important for quite a different reason, a reason which is readily understood within the field of electrochemistry. Decomposition of the electrochemical potential, $\bar{\mu}_{D^+}$, according to the formulation of Lange [8],[9]

$$\bar{\mu}_{D^+} = \mu_{D^+} + e\phi \tag{2}$$

shows that application of a difference in Galvani potential, ϕ, either within the wire (i.e. of an electrical field) or at the electrode-solution interface (i.e. of a cathodic overpotential) must lead to marked changes of the chemical potential, μ_{D^+}, i.e. of the potential energy of D^+ in the lattice [1],[3],[10]. This is the basis of the "compression" of D^+ in the lattice; we have opted in the main for the second strategy because this is the most energy efficient way of producing highly compressed D^+ in substantial volumes of the host lattice: for sufficiently high overpotentials and/or experiment durations, one would expect the charging ratio to approach unity [10],[11],[12] leading to changes in the heat of absorption of D^+ which we discuss below. It is also possible that a further phase transformation to a γ-phase takes place under these conditions [13].

Although we have opted in the main for the use of potential differences at the electrode-solution interface to achieve high compressions of D^+ in the lattice, we also note that electrodiffusion should allow one to achieve even more extreme compressions than those which can be reached in electrochemical experiments. Under special conditions one should be able to attain changes of the potential energy equivalent to the changes in kinetic energy which are the basis of investigations of "Hot Fusion". The starting point for our investigation was therefore not as far removed from the field of "Hot Fusion" as has been generally believed.

We therefore arrive at the central questions which we decided to investigate which were:

"given that D+ can be generated in a highly compressed state in Palladium host lattices and exists in a macroscopic quantum state under these conditions, would the rates of the nuclear reactions of D+ be changed compared to those observed for isolated pairs of ions?"

coupled to

"would such changes in the rates be observable?"

We observe that, whereas we expected the answer to the first question to be "yes", we also expected the answer to the second question to be "no". We decided to use in the main calorimetric measurements and the outcome of our investigations is well known: we observed excess enthalpy generation at levels

beyond those which can be explained by chemical processes, but also far above those which could be attributed to the low levels of the expected nuclear reactions [1],[14]:

$$^{2}D + {}^{2}D \rightarrow {}^{3}T(1.01\ MeV) + {}^{1}H(3.02\ MeV) \qquad (A)$$

$$^{2}D + {}^{2}D \rightarrow {}^{3}He(0.82\ MeV) + n(2.45\ MeV) \qquad (B)$$

Further work has shown (for review see e.g. [15]) that the branching ratio for reactions (A) and (B) differs markedly from unity (unity being found in "Hot Fusion") for the low levels of these particular products (ratios of T/n in the range 10^{6}-10^{9} are typically found).

We restrict attention here to one particular aspect of the investigations, the search for the conditions required for high rates of excess enthalpy generation at temperatures up to the boiling points of the electrolytes, i.e. "low-grade heat". Details of the many strange characteristics of, for example, tritium, neutron, charged particle, X- and γ-ray generation etc. can be found in the various Conference Proceedings (publications listed in [10],[11],[13] and see also [16]) as well as in reviews of the subject, e.g. [15].

Experimental

A version of the simple single compartment Dewar-type calorimetric cells in current use is illustrated in Fig 1. Heat transfer from the cells to the

surrounding water thermostats is mainly confined to radiation across the lower, unsilvered portion (the heat transfer coefficient is in fact close to that given by the product of the Stefan-Boltzmann coefficient and the radiant surface area); silvering of the top portion ensures that the system is insensitive to the level of electrolyte in the cell or the level of water in the surrounding water thermostat.

The use of a vacuum gap as the thermal impedance ensures that there is no storage of energy in this impedance, so that the resolution of time-dependent phenomena is relatively straightforward; furthermore, the systems are stable in time and all heat transfer surfaces are at uniform temperatures*. The calorimeters have a high degree of flexibility and wide dynamic range and, as we have shown [18],[19],[20], can be used at temperatures up to the boiling points of the eletrolytes+. This flexibility of the systems is of considerable importance to the present study because the experimental protocols can be made variables of the investigation (see below). We note that we have at our disposal only two state variables of the system, viz the temperature and the cell potential (or cell current) so that we can express any observable quantity (such as the rate of excess enthalpy generation) as

---

* Needless to say, the injection of heat by the electrochemical reactions and the resistive heaters used to calibrate the calorimeters is not uniform in space. However, the radial and axial mixing times are ≅3s and ≅20s respectively [17], whereas the thermal relaxation time (see equation (15)) lies between ≅4,000 and 7,000s. The calorimeters therefore behave as "well-stirred tanks".

+ We believe that much useful new information could be obtained from calorimetric measurements of electrode and cell reactions, i.e. the type of approach which we have outlined could be applied more generally.

$$Q_f = f_o[\text{electrode materials, solution composition}]f_1[E_{cell}(t),\theta(t)] \qquad (3)$$

processing variables
alloy composition

where we assume that the nature of the function f_o can be separately investigated and defined. Others have sought (and recommended, e.g. see [21]) that the function f_1 should be further restricted by using isothermal calorimetry so that the investigation is based on

$$Q_f = f_6[E_{cell}(t)] \qquad (4)$$

(for the nature of the functions f_2-f_5, see [22]). However, we must anticipate that the systems are subject to many more variables (e.g. occupation of octahedral and tetrahedral sites, steady and non-steady diffusion and migration, phase changes etc; some of these terms e.g. migration depend on products of variables) so that most of the terms of the state vectors remain "hidden" (in the sense of Lyapunov). In such a situation it is best to also make the time-dependence of the accessible variables terms of the state vectors (see especially function f_5 in [22]; the argument is analogous to the study of the time-dependence of chemical reactions). We believe that a sensible starting point for such a programme is to make the study of the temperature-time and cell potential-time series, as well as the protocols of the experiments, parts of the investigation; our wish to do so explains in part our heavy reliance on isoperibolic calorimetry and we will illustrate these aspects below.

Modelling of the Cells and Data Processing

We have shown [17],[18],[19],[22] that the "Black Box" representing the calorimeter can be modelled by the differential equation

$$C_{P,D_2O,\ell}M^0\left(\frac{d\Delta\theta}{dt}\right)=\left[E_{cell}(t)-E_{thermoneutral,bath}\right]I \quad + \quad Q_f(t)$$

rate of change in the enthalpy content of the calorimeter — rate of enthalpy input due to electrolysis — rate of excess enthalpy generation

$$+\ \Delta QH(t-t_1)-\Delta QH(t-t_2)-\frac{3I}{4F}\left[\frac{P(t)}{P^*-P(t)}\right]\left[\left(C_{P,D_2O,g}-C_{P,D_2O,\ell}\right)\Delta\theta(t)+L_{D_2O}\right]$$

calibration pulse — rate of enthalpy removal in the gas stream

$$-k_R'\left[\left(\theta_{bath}+\Delta\theta(t)\right)^4-\theta_{bath}^4\right]$$

rate of radiative heat transfer to the water bath

(5)

In arriving at this expression we have made a number of approximations, the major one being the representation of the heat transfer term

$$-k_R^0\theta_{bath}^3\left[1-\frac{(1+\lambda)It}{2FM^0}\right]\left[\frac{\left(\theta_{bath}+\Delta\theta(t)\right)^4}{\theta_{bath}^3}+4\Phi\Delta\theta(t)\right]$$

rate of heat transfer from the calorimeter

time dependent heat transfer coefficient — effect of radiation — effect of conduction

(6)

by the purely radiative term in equation (5) with an appropriate increase of the radiative heat transfer coefficient to k_R'. As we have shown elsewhere [17], this leads to a small underestimate of the heat output and, therefore, to a small underestimate of Q_f (we have sought throughout to ensure that all

approximations should lead to underestimates of Q_f). The neglect of the residual small time-dependence of the heat transfer coefficient is also justified for cells of the design shown in Fig 1, but not for the cells in use up to October 1989 which were not silvered in the top portion [17].

In order to investigate whether or not equation (5) models the calorimeters adequately, it is convenient to consider first of all the initial stages of polarisation of suitable "blank cells", e.g. containing Pt-cathodes polarised in solutions in D_2O. For such experiments we can assume

$$Q_f(t) = 0 \tag{7}$$

and, in the absence of calibrations,

$$\Delta QH(t\text{-}t_1) - \Delta QH(t\text{-}t_2) = 0 \tag{8}$$

so that the temperature-time curves should be determined by

$$C_{P,D_2O,\ell} M^0 \left(\frac{d\Delta\theta}{dt} \right) = \left[E_{cell}(t) - E_{thermoneutral,bath} \right] I - \Delta H_{evap}(t) - k_R' \left[\left(\theta_{bath} + \Delta\theta(t) \right)^4 - \theta_{bath}^4 \right] \tag{9}$$

Fig 2 gives an example of such a measurement. In the interpretation of such plots we have found it convenient to place considerable emphasis on the

"lower bound heat transfer coefficients, $(k_R')_{11}$" which, for the example illustrated follows directly from equation (9):*

$$\left(k_R'\right)_{11} = \frac{\left\{\left[E_{cell}(t) - E_{thermoneutral,bath}\right] I - \Delta H_{evap}(t) - C_{P,D_2O,\ell} M^0 \left(\frac{d\Delta\theta}{dt}\right)\right\}}{\left[\left(\theta_{bath} + \Delta\theta(t)\right)^4 - \theta_{bath}^4\right]} \tag{10}$$

Such values are determined point-by-point with $d\Delta\theta/dt$ being given by the second order forward difference. In order to reduce the effects of random fluctuations it is also convenient to consider the 11-point running mean of $\left(k_R'\right)_{11}$ which is equivalent to

$$\overline{\left(k_R'\right)_{11}} = \frac{\left\{\left[\overline{E_{cell}(t)} - E_{thermoneutral,bath}\right] I - \overline{\Delta H_{evap}(t)} - C_{P,D_2O,\ell} M^0 \left(\overline{\frac{d\Delta\theta}{dt}}\right)\right\}}{\left[\left(\theta_{bath} + \overline{\Delta\theta(t)}\right)^4 - \theta_{bath}^4\right]} \tag{11}$$

Needless to say, in the presence of a calibration pulse, the term $\Delta QH(t\text{-}t_1) - \Delta QH(t\text{-}t_2)$ must be included in the numerators of equations such as (10) or (11).

A major reason for our emphasis on the use of $(k_R')_{11}$ is the fact that this heat transfer coefficient is independent of any method of calibration such as the "square wave heating pulse". The errors in $(k_R')_{11}$ therefore give us the precision of the measurements (although it could well be argued that for "blank experiments" these errors also give us the accuracy). We have found that the relative standard deviation of such point-by-point estimates is ≅0.1%

* This "lower bound heat transfer coefficient was originally designated as $(k_R')_1$ (as it was the first coefficient investigated). The designation was later changed to $(k_R')_{i,1}$ where the suffix "i" denotes particular ways of making the estimates, e.g. see $(k_R')_{31}$ below.

[18],[19]; it is not surprising that this can be reduced by using the whole data set, for example by taking the integrals of all the terms in equation (9):

$$\frac{\left\{\int_0^t [\text{Enthalpy input } (\tau)]d\tau - \int_0^t \left[\Delta H_{evap}(\tau)\right]d\tau\right\}}{\int_0^t \left[(\theta_{bath} + \Delta\theta(\tau))^4 - \theta_{bath}^4\right]d\tau}$$

$$= \left(k_R'\right)_{31} + \frac{C_{P,D_2O,\ell}M^0[\Delta\theta(t) - \Delta\theta(0)]}{\int_0^t \left[(\theta_{bath} + \Delta\theta(\tau))^4 - \theta_{bath}^4\right]d\tau} \qquad (12)$$

Fig 3 illustrates a test of equation (12); we have found that the use of prolonged sections of the time series allows us to decrease the relative standard deviations to ≅0.01% [18],[19],[22] and we will comment below on the importance of seeking to make the measurements and interpretations at such high levels of precision*.

The reason why $(k_R')_{11}$ is always a lower bound is because the neglect of any rate of excess enthalpy generation, equation (7), inevitably reduces this heat transfer coefficient from the true value. However, in this case the time-dependence of $(k_R')_{11}$ in turn reflects the time-dependence of Q_f: indeed, one can frequently use the maximum value of $(k_R')_{11}$ to make semi-quantitative estimates of the "lower bound rates of excess enthalpy generation, $(Q_f)_{11}$" [18],[19]. It is naturally preferable to calibrate the systems using the resistive heaters. One approach is to make a thermal balance at the single point (θ_2,t_2)

* The fitting of equations such as (12) can be done using linear regression. The calorimeters in use up to October 1989 were not silvered in their top portions so that the time-dependence of the heat transfer coefficients was appreciable, cf equation (6). These early data sets were fitted to the numerical integrals of equations such as (5) using non-linear regression; the precision and accuracy achieved were comparable to that in our current work. We will comment further elsewhere on the applicability of linear, multi-linear and non-linear regression methods (see also [22]).

shown in the schematic diagram, Fig 4. We have designated such "true" heat transfer coefficients $(k_R')_2$ (this was the second method we adopted*) given by

$$\left(k_R'\right)_2 = \frac{\left\{\left[E_{cell}(\Delta\theta_1, t_2) - E_{cell}(\Delta\theta_2, t_2)\right]I + \Delta Q - \Delta H_{evap}(\Delta\theta_2, t_2) + \Delta H_{evap}(\Delta\theta_1, t_2) - C_{P,D_2O,\ell}M^0\left(\frac{d\Delta\theta}{dt}\right)_{(\Delta\theta_2,t_2)} + C_{P,D_2O,\ell}M^0\left(\frac{d\Delta\theta}{dt}\right)_{(\Delta\theta_1,t_2)}\right\}}{\left[\left(\theta_{bath} + \Delta\theta_2\right)^4 - \left(\theta_{bath} + \Delta\theta_1\right)^4\right]} \tag{13}$$

Values of $(k_R')_2$ are accurate at about the 1% level. This accuracy can be increased to ≅0.1% by using long sections of the time series using an approach analogous to that leading to equation (12):

$$\left(k_R'\right)_{22} = \frac{\left\{\int_0^t [\text{Enthalpy input } (\tau)]\,d\tau - [\text{Enthalpy input } (0)]t - \int_0^t \left[\Delta H_{evap}(\tau)\right]d\tau + \left[\Delta H_{evap}(0)\right]t + \Delta Q\, t - C_{P,D_2O,\ell}M^0[\Delta\theta(t) - \Delta\theta(0)]\right\}}{\left\{\int_0^t \left[\left(\theta_{bath} + \Delta\theta(\tau)\right)^4 - \theta_{bath}^4\right]d\tau - \left[\left(\theta_{bath} + \Delta\theta(0)\right)^4 - \theta_{bath}^4\right]t\right\}} \tag{14}$$

where we have designated the origin as (Δθ(0),0).

---

* This is the method of calibration advocated by Wilson et al [23] in a critique of our publication [17]. However, as we made clear in Appendix 4 of [17], we carried out a thermal balance at a point just preceding t_1 and not at the point t_2. The heat transfer coefficient required for the balance at t_1 is defined as (k_4') in [24]. Values of $(Q_f)_4$ based on $(k'_R)_4$ are slightly lower than those of $(Q_f)_2$ based on $(k_R')_2$ (however, see comments on "positive feedback" below).

Apart from the usefulness of $(k_R')_2$ and $(k_R')_{22}$ in estimating $(Q_f)_2$ for cells containing Pd-cathodes polarised in D_2O solutions, estimates of $(Q_f)_2$ for "blank experiments" also allow us to put a limit on side reactions which might lead to the generation of an apparent excess enthalpy term. We have found that $(k_R')_2$ is very slightly larger than $(k_R')_{11}$ for such "blank experiments" consistent with the generation of 1-2 mW of excess power. The suggestion that the observed rates of excess enthalpy generation can be attributed to recombination of D_2 and O_2 in the cells (based on a proposal by Kreysa et al [25]) can be discounted*.

Results and Discussion

Contrary to the views which have frequently been expressed, it is not very difficult to demonstrate the early generation of low levels of excess enthalpy for Pd and Pd-based cathodes polarised in 0.1M LiOD in D_2O provided the calorimetric system has sufficient precision and accuracy. For Pd and Pd-based cathodes it is found that $(k_R')_{11}$ is initially negative, Fig 5A, due to the neglect of the exothermic absorption of deuterium in the lattice. This result is not as dramatic as appears at first sight because the numerator of equation (10) tends to zero as $t \rightarrow 0$: $(k_R')_{11}$ is therefore especially sensitive to excess enthalpy terms in this region of time. This result is also obtained for Pd and Pd-based cathodes polarised in 0.1M LiOH in H_2O, but for these systems $(k_R')_{11}$ then increases to reach the true value $(k_R')_2$. By contrast, for

* We note that there are no exposed metal surfaces in the head spaces of our cells, Fig 1. Reoxidation of H_2 does not take place at oxide coated Pt-anodes; the reduction of dissolved O_2 is diminished by the degassing of the solution in the vicinity of the cathodes due to deuterium evolution.

experiments in D_2O solutions, $(k_R')_{11}$ frequently passes through a maximum and $(k_R')_{11}$ never reaches $(k_R')_2$. It follows that a further process (or further processes) leading to excess enthalpy generation are established. The experiments we conduct are based on regular refilling of the cells every two days to make up for losses due to electrolysis and, over this duration, rates of excess enthalpy generation in the range 1-4% of the enthalpy inputs can frequently be observed. Fig 6 illustrates the cumulative excess enthalpy for one such experiment; the excess enthalpy due to the exothermic absorption and the further excess enthalpy generation can clearly be discerned. The importance of such observations is two-fold: first, we observe that these excess enthalpies are in the range 10-30σ based on the accuracy of the heat transfer coefficients and 100-300σ based on the precision (as we have noted above, one can make a strong case for basing such estimates on the precision rather than the accuracy); secondly, we note that the total excess enthalpies over such a two-day period can reach $\cong$1MJ (mole Pd)$^{-1}$. Already at this stage, therefore, we are faced with the dilemma of explaining energies which are outside the range of known chemical and physical processes.

The larger values of the excess enthalpies which we reported [1],[17] (and which have also been reported by other research groups) have been based on prolonged polarisations of the cathodes (periods up to $\cong$3 months). Table 1 lists some values observed prior to March 1989 which we took as a basis of our view that excess enthalpy generation takes place in the bulk of the cathodes.* We believe that the majority of the investigators who have reported

* The excess enthalpies listed in Table 1 must be judged in the context of a variety of "blank experiments" which give a thermal balance at the ±1-3 mW level. Such "blanks" include Pt-cathodes polarised in H_2O and D_2O solutions, Pd-cathodes polarised in H_2O solutions as well

"positive results" have been unable to detect the lower levels of excess enthalpy generation during the initial stages of the experiments (or else have failed to look for these effects).

Our further early work indicated that there is an apparent threshold in the current density in the range 50-100mA cm^{-2} below which excess enthalpy cannot be observed [17] (for other interesting comments on this phenomenon see [11],[12] and the review [15]). An effect which was of special importance in the development of this project was the observation of "bursts" in the rates of excess enthalpy production and, of these, the one illustrated in Figs 7A, B and C was of special significance [17]. This phenomenon was both remarkable and unremarkable: it was unremarkable because the rates of excess enthalpy generation reached (say 15W cm^{-3}) were within our range of observations of the "normal" phenomenon (say 10^{-2}-10^{2}W cm^{-3} for I in the range 50-1000mA cm^{-2}); it was remarkable because it was observed at a relatively early stage of the experiment (≅18 days after the start of polarisation), itself lasted ≅18 days and led to a total output some 8 times larger than the total energy input. Moreover, the cumulative output, Fig 7C, (say ≅130MJ $(mole\ Pd)^{-1}$) was quite outside the range of chemical or conventional physical processes.* Furthermore, such observations raised the prospect of sustained efficient energy production at technologically useful temperatures: it must be borne in

---

as Pd-cathodes polarised in D_2O solutions but which do not show any excess enthalpy generation [17].

* We termed our early observations of such effects "unexplained rises in the cell temperatures". Such "unexplained rises" have also been observed by other research groups including one whose members concluded that there was no excess enthalpy generation. However, we believe that one can only explain such observations by either excess enthalpy generation or, in extremis, malfunction of the instrumentation. It is not possible to conclude that the instruments are functioning correctly, yet that there is no excess enthalpy generation.

mind that the calorimetric systems used in the research are highly energy-inefficient because of the low electrolyte concentration, the relatively large anode-cathode spacing and the use of oxygen evolution as the counter electrode reaction.

One key to seeking an explanation for the increases in the rates of excess enthalpy production lies in the detailed examination of the temperature-time and associated cell potential-time plots used to derive $(k_R')_2$ and $(k_R')_{11}$ which we illustrate here with Figs 8A-C. For early stages of the experiments, Fig 8A, we find the expected "normal" behaviour. The temperature-time curve following the application of the calibration pulse ΔQ shows the expected relaxation with a relaxation time (see Appendix 4 of [17])

$$\tau \cong \frac{C_{P,D_2O,\ell} M^0}{\left[4k_R' \theta_{bath}^3 - \left(\frac{dE_{cell}}{d\Delta\theta} \right) I \right]} \qquad (15)$$

We find $(k_R')_2$ (at $(\Delta\theta_2,t_2)$) > $(k_R')_{11}$ (at t_1) and a small positive value of $(Q_f)_2$ (at $(\Delta\theta_1,t_2)$), i.e. the results are entirely as expected. However, with more prolonged polarisation, Fig 8B, we reach a pattern of behaviour which is, at first sight, completely anomalous. The perturbation now does not relax according to (15): the temperature continues to increase with time so that there must be an enthalpy generating process which also increases with time. We find that $(k_R')_2$ (at $(\Delta\theta_2,t_2)$) < $(k_R')_{11}$ (at t_1) and, inevitably $(Q_f)_2$ (at $(\Delta\theta_1,t_2)$) is negative, i.e. the cell is apparently behaving as a refrigerator! Furthermore, the "cooling curve" is anomalous (we note that this is a special case of the effect of "Heat after Death" [20]) and, at long times, the cell temperature increases

yet the energy input decreases. At still later stages, Fig 8C, we revert to the normal behaviour observed in Fig 8A except that $(Q_f)_2$ (at $(\Delta\theta_1,t_2)$) has now increased.

We believe that the explanation of the behaviour illustrated in Fig 8B can only be in terms of "positive feedback": the increase in temperature caused by the application of the calibration pulse ΔQ induces an increase in Q_f. In consequence, $\Delta\theta_{cell}$ increases to a level it would not attain if there were no "positive feedback" and $(k_R')_2$ (at $(\Delta\theta_2,t_2)$) < $(k_R')_{11}$ (at t_1) etc. Such intervention of "positive feedback" is entirely reasonable when viewed in the context of extrapolations of the known variation of the heat of absorption of hydrogen in palladium with the charging ratio, Fig 9 [26]. Measurements of the rates of excess enthalpy production as a function of the charging ration [11],[12] show that the "threshold" is in the region in which the aborption of D in the lattice changes from being exothermic to being endothermic. Once this process has become endothermic, any increase in the cell temperature, such as those due to the application of the heater calibration pulse, must lead to further increases in the charging ratio and, therefore, of the rates of excess enthalpy production. This is one mechanism which can be at the root of the phenomenon of "positive feedback", Fig 8B, although it is not clear as yet whether the change in sign of the heat of absorption is the only reason for the observation of this effect. We note also that there could be several explanations for the changes in the thermodynamics of absorption. One such explanation is the presence of a further phase transformation to a γ-phase at high charging ratios [13]. Such a phase transformation would explain the marked oscillations in cell potential and/or cell temperature which are

observed in this region, Fig 10A and B, although the mere fact of the transition through a region of zero heat of absorption is sufficient reason for expecting large fluctuations in the systems variables. We note that Pd-Rh alloys are especially prone to show such oscillatory behaviour, although it is shown to some extent by all Pd-based cathodes (including Pd itself). The oscillations vary in amplitude and frequency and can be regular or irregular so that the search for explanations of the effects will have to include a search for the characterisation and explanation of the strange attractor(s) which may be the basis of the observed effects.

One feature which is of special importance to the topic of this report is that prolonged maintenance of the electrodes in this transition region reduces (or, in the limit can destroy) the phenomenon of excess enthalpy generation. It is therefore essential to "drive the system" through the transition region and this is one of the major reasons why the protocols of the experiments become one of the variables of the investigation.

We note also that the measurements show other features to be expected for a transition from exothermic to endothermic absorption. Thus the increase in the rate of excess enthalpy generation due to the application of the heater calibration pulse, Fig 8B, may be accompanied by a transient endothermic process just as termination of the calibration may be accompanied by a transient exothermic effect. These are phenomena which we will discuss elsewhere. As far as the main theme of this report is concerned, it is the transition from exothermic to endothermic absorption which must lead to an increase in the charging ratio with increase of the temperature and the

maintenance of high charging ratios at "intermediate temperatures", say, up to the boiling points of the electrolytes. In consequence, the rates of excess enthalpy production increase and it becomes possible to observe the production of such "low-grade heat".

Cells of the type shown in Fig 1 are not well-suited to making calorimetric measurements near the boiling points, but they do at least allow the timing of the evaporation of the cell contents, Fig 11 (boiling to dryness). Application of equations related to (5) allows us to attempt conservative interpretations. Although such equations do not contain any adjustable parameters (and we note again that (5) provides an exact model of the calorimeters), we can impose a degree of flexibility by adjusting the barometric pressure. We can therefore base a conservative interpretation on the questions: "what barometric pressure do we have to assume to allow the total evaporation of the D_2O without invoking the phenomenon of boiling?" coupled to "what is the time-dependence of the rate of excess enthalpy generation required to explain the evaporation?" Fig 11 gives an example of such a calculation. For an assumed atmospheric pressure of 0.953 bar, the rate of excess enthalpy production would have had to increase to $\cong 370 Wcm^{-3}$ to explain evaporation to dryness. However, such an explanation would have required the cell to be half-full some 2.3 hours before termination of electrolysis, whereas visual observation showed this stage to be reached $\cong$11 minutes before dryness. Use of a barometric pressure of 0.97 bar gives the other time course of the rate of excess enthalpy generation which is more closely in line with the visual observations. We note also that the observed barometric pressure was 0.966 bar and it is reasonable to assume that the pressure in the cell was somewhat

higher than this due to compression in the gas vent. We see that this particular explanation requires the rate of excess enthalpy generation to have reached ≅ 4kWcm^{-3} at the end of electrolysis. Fig 5B gives the variation of $(k_R')_{11}$ with time required for the two extrema of the explanations and we can see that both require $(k_R')_{11}$ to become negative, i.e. any conventional explanation would require a spontaneous flow of heat from the water bath (at 20°C) into the cell (at 100°C). Needless to say, this is beyond the realms of possibility.

At this stage we must conclude that the actual behaviour must lie between the extrema and, evidently, much closer to the second than the first. This therefore raises the possibility that it is possible to use such systems for the generation of high levels of low-grade heat; part of our current research is concerned with the exploration of the parameter space at the boiling points.

References

1. M. Fleischmann, S. Pons and M. Hawkins, J. Electroanal. Chem., 261, 301 (1989); for some corrections see J. Electroanal. Chem., 263, 187 (1989).

2. M. Fleischmann, S. Pons and G. Preparata, Nuovo Cimento, 107A (1994).

3. Claudia Bartolomeo, M. Fleischmann, G. Larramona, S. Pons, Jeanne Roulette, H. Sugiura and G. Preparata, "Alfred Coehn and After: the α,β,γ of the Palladium-Hydrogen System" Proceedings of the 4th International Conference on Cold Fusion, Maui, Hawaii, U.S.A. (December 6-9, (1993)); EPRI TR-104188-VI page 19-1; Fusion Technology, in the press.

4. A. Coehn, Z. Elektrochem., 35, 676 (1929).

5. C. Wagner and G. Heller, Z. Physik. Chem., B46, 242 (1940).

6. H. Wipf, Chapter 7 in G. Alefeld and J. Völkl, *"Hydrogen in Metals II"* Springer Verlag, Berlin, Heidelberg, New York (1978) ISBN 3-540-0883-0; 0-387-08883-0.

7. B. Dandapani and M. Fleischmann, J. Electroanal. Chem., 39, 323 (1972).

8. E. Lange and K. P. Miscenko, Z. Phys. Chem., 149, 1 (1930).

9. E. Lange, Z. Elektrochem., 55, 76 (1951).

10. M. Fleischmann, "An Overview of Cold Fusion Phenomena", Proceedings of the 1st Annual Conference on Cold Fusion, Salt Lake City, Utah, U.S.A., March 1990.

11. M. C. H. McKubre, S. Crouch-Baker, A. M. Riley, S. I. Smedley and F. L. Tanzella, "Excess Power Observations in Electrochemical Studies of the D/Pd System: the Influence of Loading" in *"Frontiers of Cold Fusion"*, Ed. H. Ikegami, Proceedings of the 3rd International Conference on Cold Fusion, Nagoya, Japan, October 21-25 (1993); Universal Academy Press Inc., Tokyo, Page 5 (1993); ISSN 0915-8502.

12. K. Kunimatsu, H. Hasegawa, A. Kubota, N. Imai, M. Ishikawa, H. Akita and Y. Tsuchida, "Deuterium Loading Ratio and Excess Heat Generation during Electrolysis of Heavy Water by a Palladium Cathode in a Closed Cell Using a Partially Immersed Fuel Cell Anode", in *"Frontiers of Cold*

Fusion", Ed. H. Ikegami, Proceedings of the 3rd International Conference on Cold Fusion, Nagoya, Japan, October 21-25 (1993); Universal Academy Press Inc., Tokyo, page 31 (1993); ISSN 0915-8502.

13. G. Preparata, "Towards a Theory of Cold Fusion Phenomena", Ed. B. Stella, Proceedings of the Rome Workshop on Cold Fusion, February (1993).

14. M. L. Oliphant, P. Harteck and Lord Rutherford, Nature, 133, 413 (1934).

15. E. Storms, "Review of Experimental Observations about the Cold Fusion Effect", Fusion Technology, 20, 433 (1991).

16. Proceedings of the 2nd International Conference on Cold Fusion, Como, Italy, June 29 - July 4 (1991), Eds. T. Bressani, E. Del Giudice and G. Preparata, "The Science of Cold Fusion", Conference Proceedings, The Italian Physical Society, Bologna, Italy, 33 (1992); ISBN 887794-045-X.

17. Martin Fleischmann, Stanley Pons, Mark W. Anderson, Lian Jun Li and Marvin Hawkins, J. Electroanal. Chem., 287, 293 (1990).

18. Martin Fleischmann and Stanley Pons in *"Frontiers of Cold Fusion"*, Ed. H. Ikegami, Proceedings of the 3rd International Conference on Cold Fusion, Nagoya, Japan, October 21-21 (1993); Unversal Academy Press Inc., Tokyo, page 47 (1993); ISSN 0915-8502.

19. Martin Fleischmann and Stanley Pons, Phys. Lett. A, 176, 118 (1993).

20. S. Pons and M. Fleischmann, "Heat after Death" Proceedings of the 4th International Conference on Cold Fusion, Maui, Hawaii, U.S.A. (December 6-9, (1993)); EPRI TR-104188-VI page 8-1; Fusion Technology, in the press.

21. D. Morrison, Messages on the Electronic Mail Networks.

22. M. Fleischmann, S. Pons, Monique Le Roux and Jeanne Roulette, "Calorimetry of the Pd-D_2O System: the Search for Simplicity and Accuracy" Proceedings of the 4th International Conference on Cold Fusion, Maui, Hawaii, U.S.A. (6-9 December 1993); EPRI TR-104188-V1 page 1-1, Fusion Technology: in the press.

23. R. H. Wilson, J. W. Bray, P. G. Kosky, H. B. Vakil and F. G. Will, J. Electroanal. Chem., 332, 1 (1992).

24. M. Fleischmann and S. Pons, J. Electroanal. Chem., 332, 33 (1992).

25. G. Kreysa, G. Marx and W. Plieth, J. Electroanal. Chem., 266, 437 (1989).

26. T. B. Flanagan and J. F. Lynch, J. Phys. Chem., 79, 444 (1975).

Legends for Figures

Fig 1: Schematic diagram of the single compartment open Dewar-type calorimetric cells in current use.

Fig 2: The temperature-time and cell potential-time curves for the first two days of polarisation of a Pt-cathode in 0.1M LiOD in D_2O. Electrode dimensions: 1.5mm diameter, 12.5mm length; cell current: 200mA.

Fig 3: the fit of the experimental data shown in Fig 2 to equation (12) over the time interval 49,500 to 172,000s. Intercept $0.82462 \times 10^{-9} WK^{-4}$; Slope $458.8 JK^{-1}$; correlation coefficient 0.99999+.

Fig 4: Schematic diagram of the methodology used to evaluate $(k_R')_{11}$ and $(k_R')_2$

Fig 5A: Plot of the lower bound heat transfer coefficient $(k_R')_{11}$ as a function of time for the initial stage of the polarisation of a Pd-cathode in 0.1M LiOD in D_2O. Electrode dimensions: 2mm diameter, 12.5mm length; cell current: 200mA.

Fig 5B: Plots of the lower bound heat transfer coefficients $(k_R')_{11}$ as a function of time for the last stage of the polarisation of the same Pd-cathode in 0.1M LiOD in D_2O. Cell current: 500mA.

Fig 6: The variation with time of the total excess enthalpy generated during the first two days of polarisation of a Pd-cathode in 0.1M LiOD in D_2O. Electrode dimensions: 2mm diameter, 12.5mm length; cell current: 200mA.

Fig 7A: Cell temperature-time and cell potential-time plots for the polarisation of a Pd-cathode in 0.1M LiOD in D_2O. Electrode dimensions: 4mm diameter, 12.5mm length; current density 64mA cm^{-3}; bath temperature 29.87°C.

Fig 7B: The rate of excess enthalpy generation for the experiment illustrated in Fig 7A.

Fig 7C: The total specific excess enthalpy as a function of time for the experiment illustrated in Figs 7A and 7B.

Fig 8A: Temperature-time and cell potential-time curves for the polarisation of a Pd90 Ag10 electrode in 0.1M LiOD in D_2O before the onset of "positive feedback". Electrode dimensions: 4mm diameter, 12.5mm length; cell current: 500mA.

Fig 8B: The temperature-time and cell potential-time curves for the system illustrated in Fig 8A but during the stage of "positive feedback".

Fig 8C: The temperature-time and cell potential-time curves for the system illustrated in Figs 8A and 8B but after the completion of the stage of "positive feedback".

Fig 9: The variation of the relative partial molar enthalpy of absorption of hydrogen in palladium as a function of the charging ratio.

Fig 10A: Temperature-time and cell potential-time curves for the polarisation of a Pd90 Rh10 cathode in 0.1M LiOH in H_2O. Electrode dimensions: 1mm diameter, 12.5mm length; cell current: 200mA.

Fig 10B: Expanded section of Fig 10A.

Fig 11: The variation of the specific excess enthalpy with time for the last stage of polarisation of the system illustrated in Figs 5A and 5B. The assumptions for the two plots shown are given in the text.

Table 1. Initial Measurements of the Specific Excess Enthalpy Generated in Pd-rod cathodes.

Rod Dimensions & Material	I	E_{cell}	θ_{cell}	Joule Heat Out	Joule Heat In	Excess Enthalpy	Excess Specific Enthalpy
Ø x Length /cm	/mA cm^{-2}	/V	/°C	/watt	/watt	/watt	/watt cm^{-3}
Pd							
0.1 x 10	64	3.637	32.83	0.462	0.419	0.042	0.53
0.2 x 10	64	4.139	37.78	1.163	1.040	0.123	0.39
0.4 x 10	64	5.137	48.25	3.38	2.88	0.5	0.40
0.1 x 1.25	512	9.08	40.49	1.67	1.51	0.17	17.3
0.2 x 1.25	512	8.25	49.70	3.34	2.68	0.66	16.8
0.4 x 1.25	512	8.66	70.54	7.88	5.70	2.18	13.9

All data taken in 0.1M LiOD inD_2O of 99.5% isotopic purity.

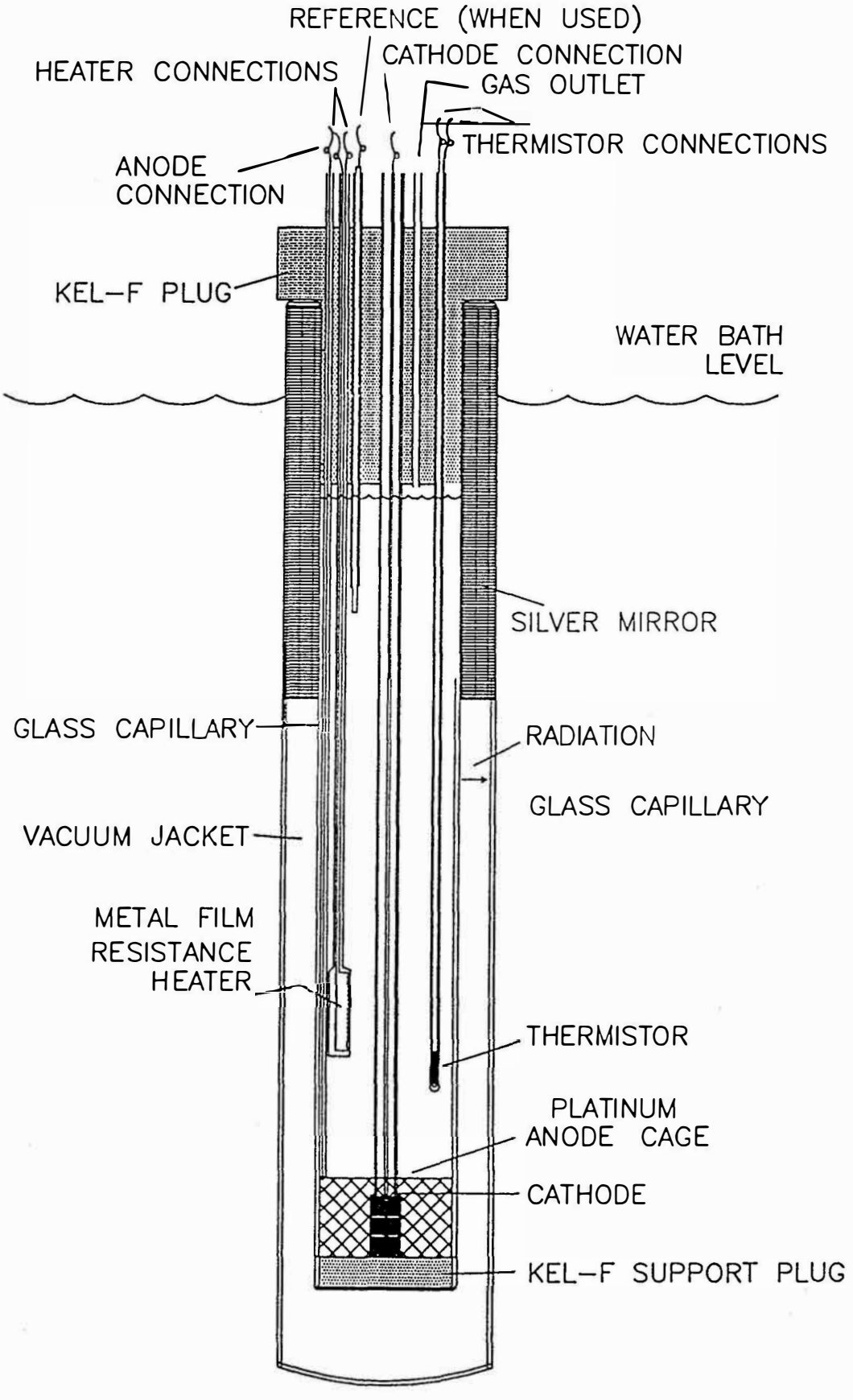

Fig 1: Schematic diagram of the single compartment open Dewar-type calorimetric cells in current use.

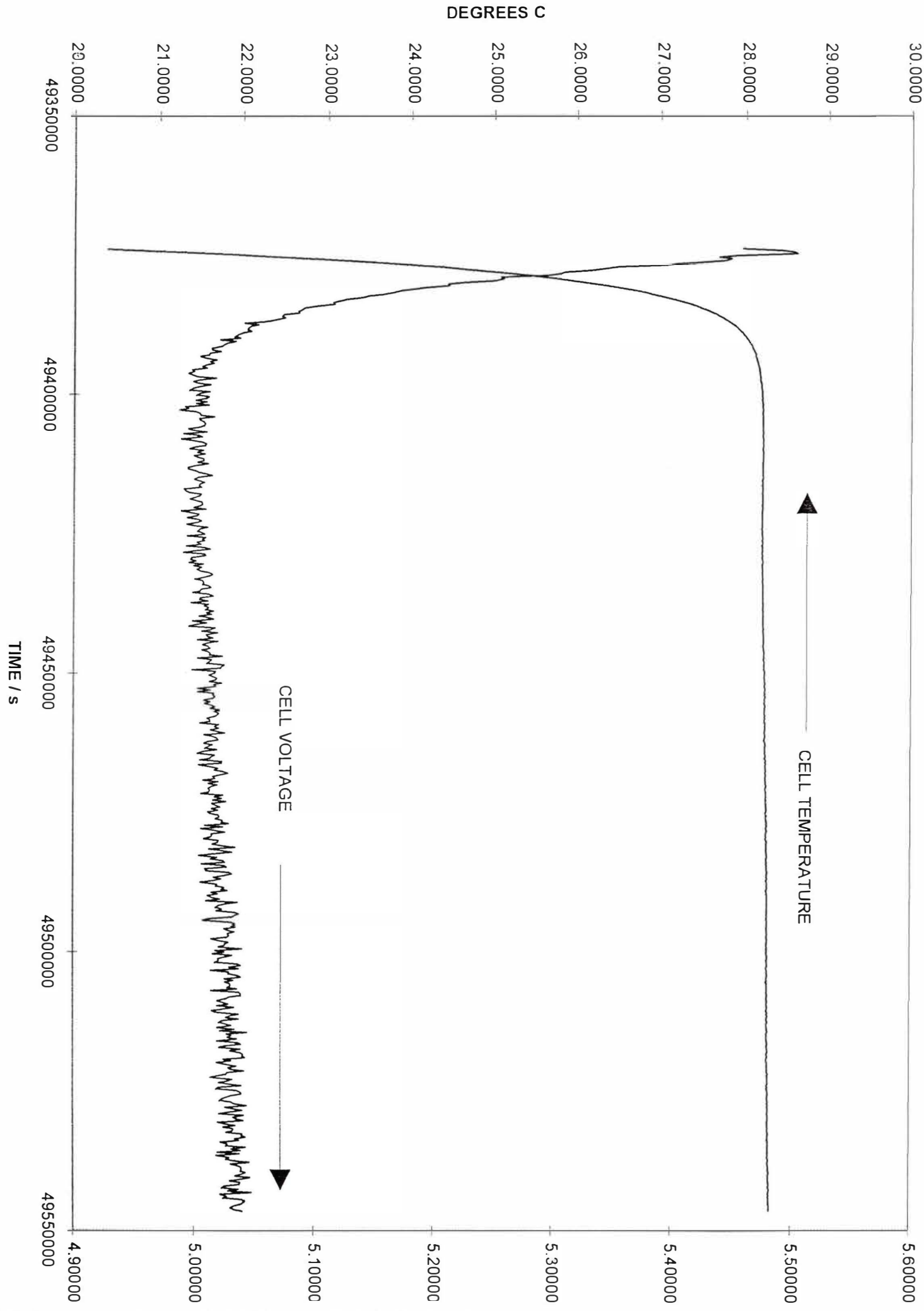

Fig 2: The temperature-time and cell potential-time curves for the first two days of polarisation of a Pt-cathode in 0.1M LiOD in D_2O. Electrode dimensions: 1.5mm diameter, 12.5mm length; cell current: 200mA.

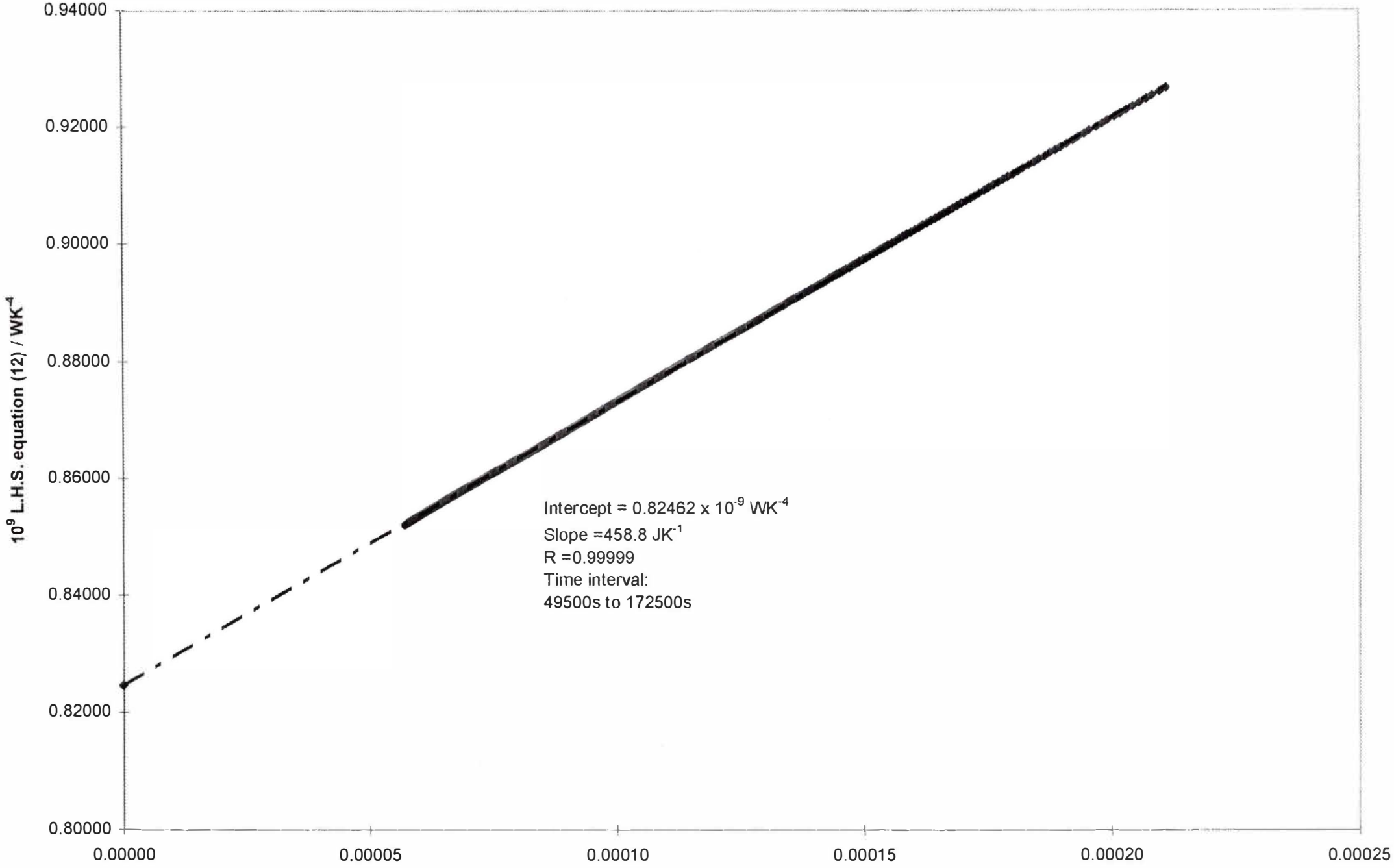

Fig 3: the fit of the experimental data shown in Fig 2 to equation (12) over the time interval 49,500 to 172,000s. Intercept 0.82462 × $10^{-9}WK^{-4}$; Slope 458.8JK^{-1}; correlation coefficient 0.99999+.

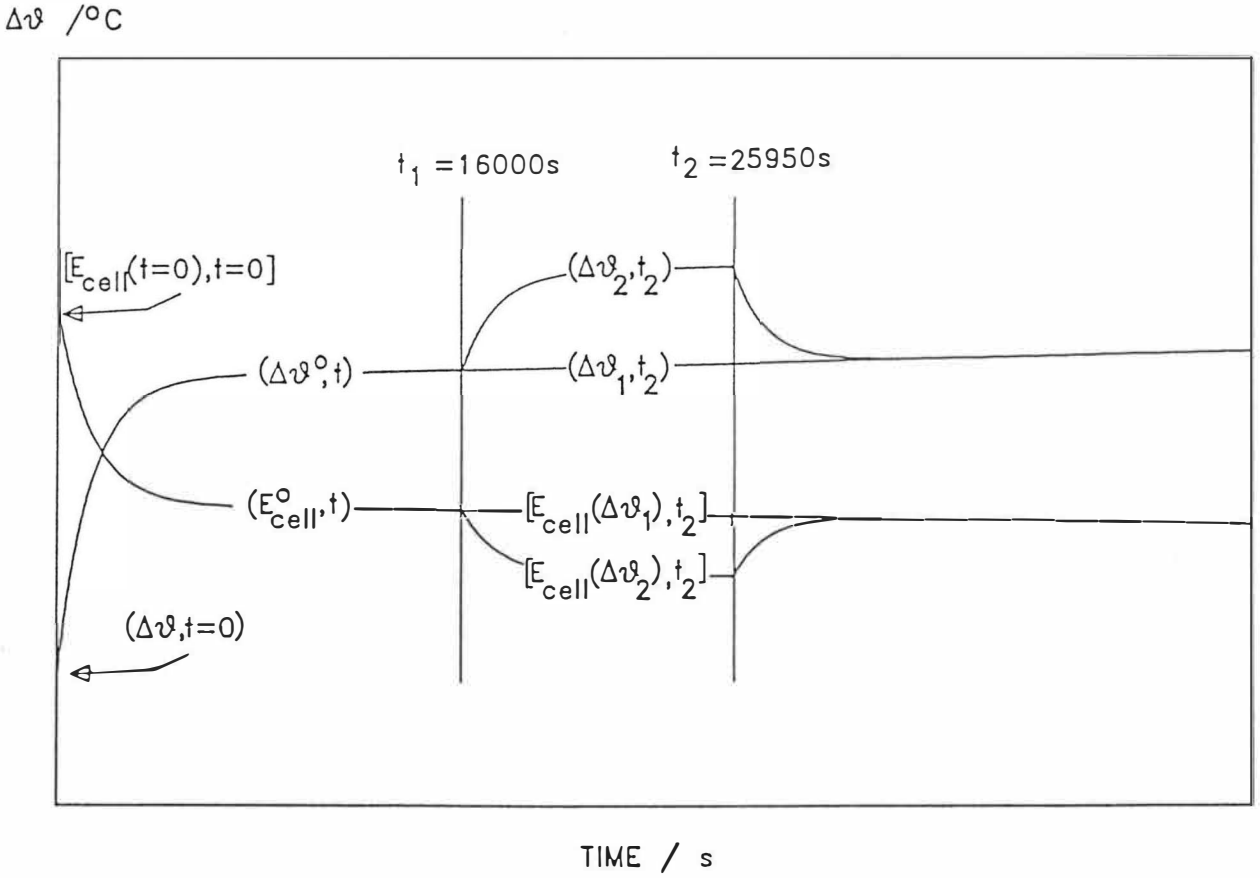

Fig 4: Schematic diagram of the methodology used to evaluate $(k_R')_{11}$ and $(k_R')_2$

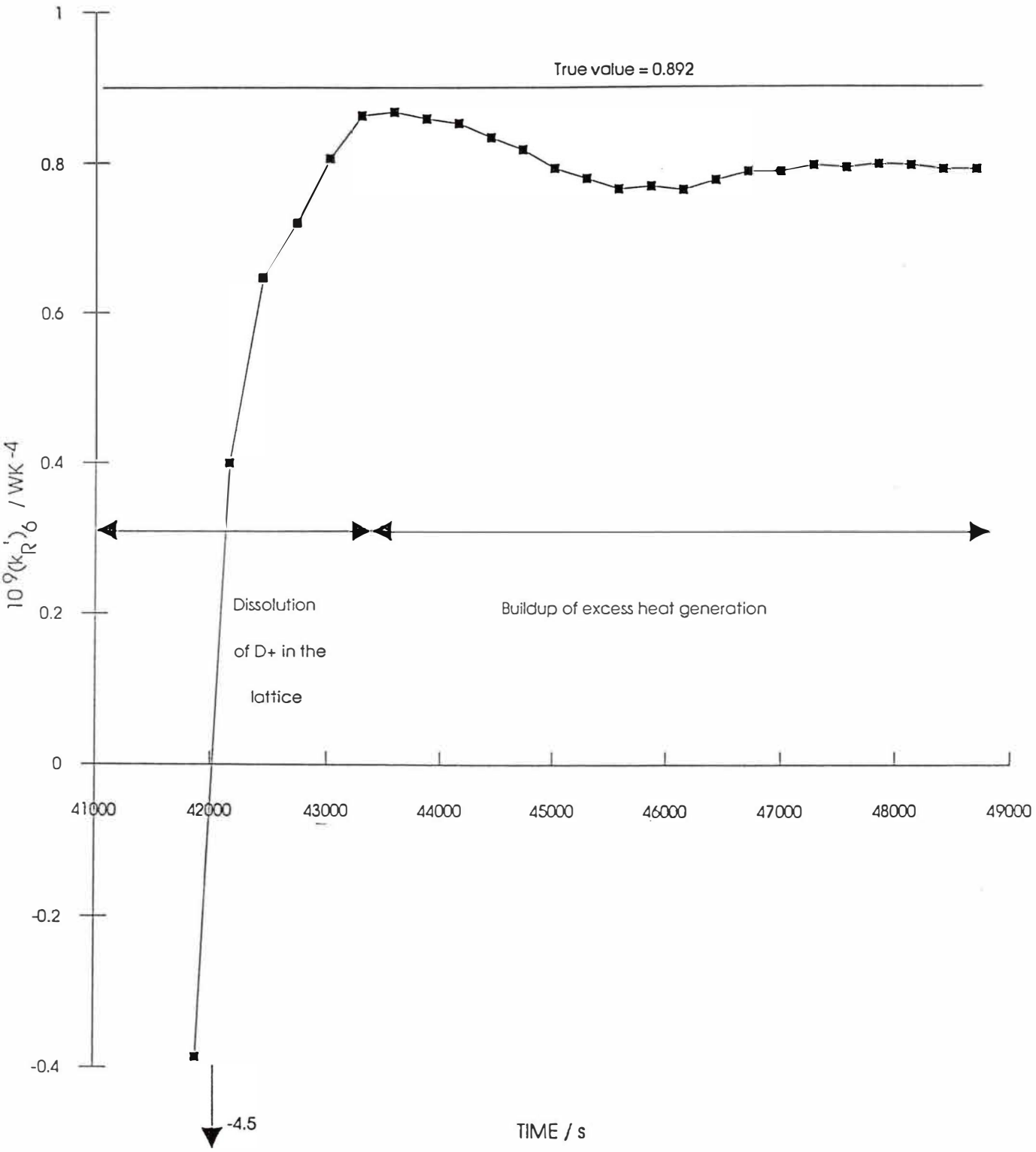

Fig 5A: Plot of the lower bound heat transfer coefficient $(k_R')_{11}$ as a function of time for the initial stage of the polarisation of a Pd-cathode in 0.1M LiOD in D_2O. Electrode dimensions: 2mm diameter, 12.5mm length; cell current: 200mA.

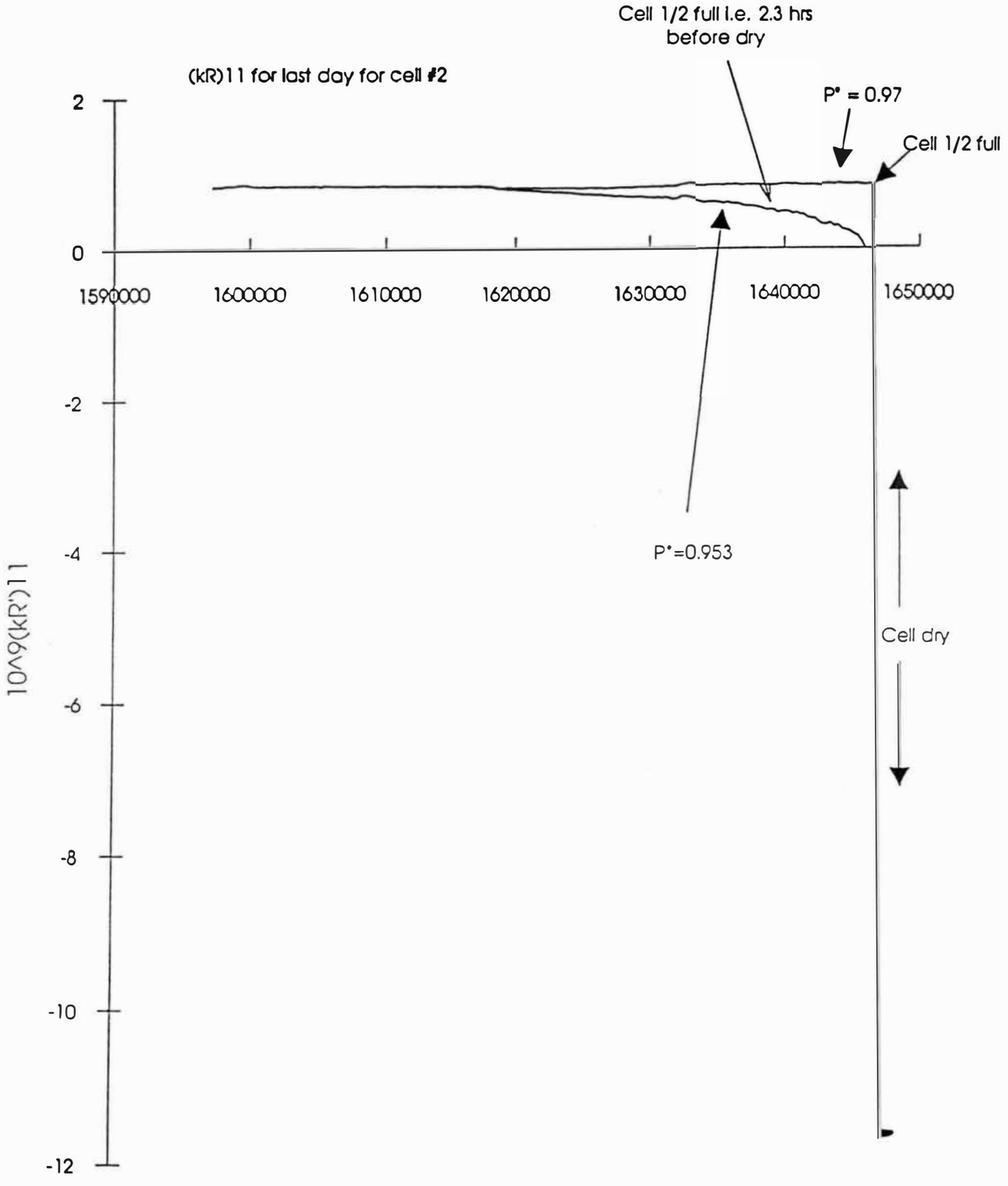

Fig 5B: Plots of the lower bound heat transfer coefficients $(k_R')_{11}$ as a function of time for the last stage of the polarisation of the same Pd-cathode in 0.1M LiOD in D_2O. Cell current: 500mA.

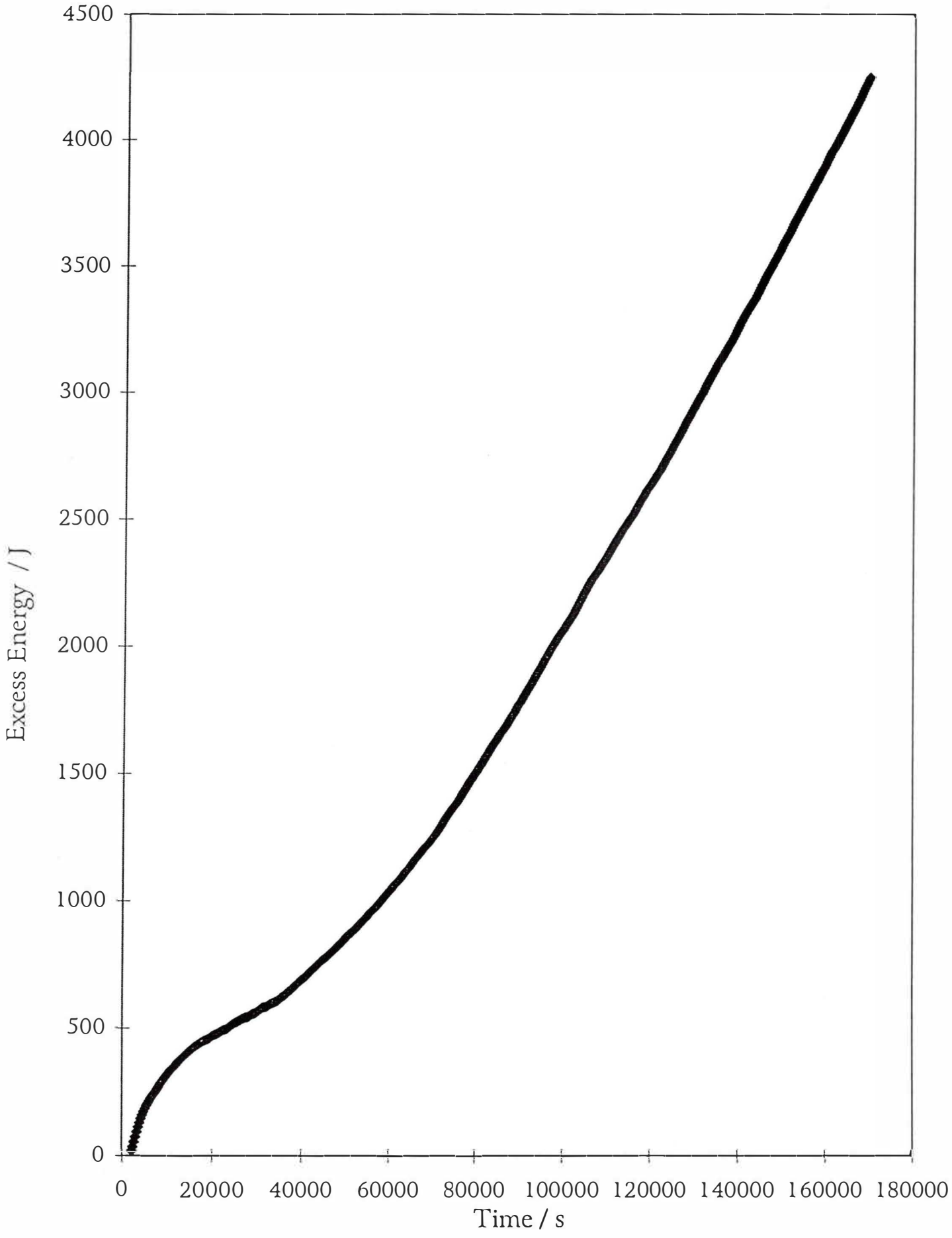

Fig 6: The variation with time of the total excess enthalpy generated during the first two days of polarisation of a Pd-cathode in 0.1M LiOD in D_2O. Electrode dimensions: 2mm diameter, 12.5mm length; cell current: 200mA.

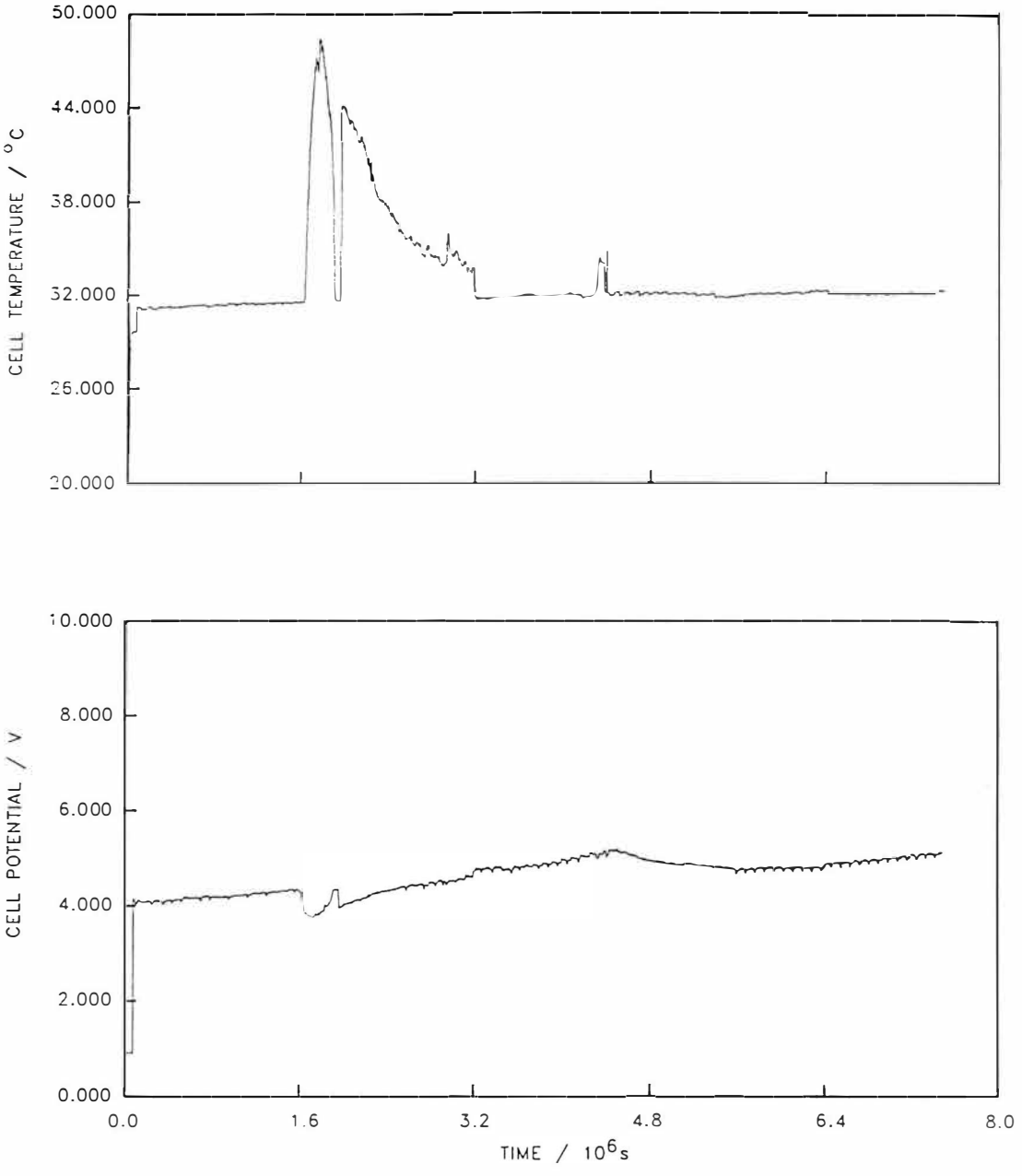

Fig 7A: Cell temperature-time and cell potential-time plots for the polarisation of a Pd-cathode in 0.1M LiOD in D_2O. Electrode dimensions: 4mm diameter, 12.5mm length; current density 64mA cm^{-3}; bath temperature 29.87°C.

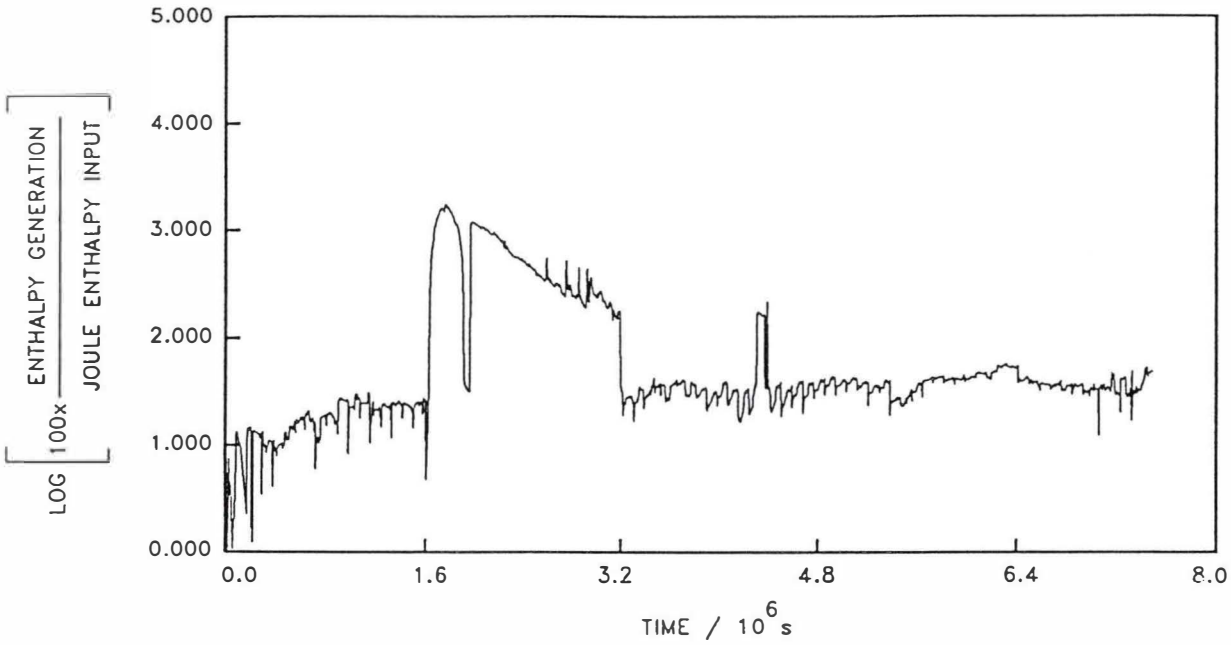

Fig 7B: The rate of excess enthalpy generation for the experiment illustrated in Fig 7A.

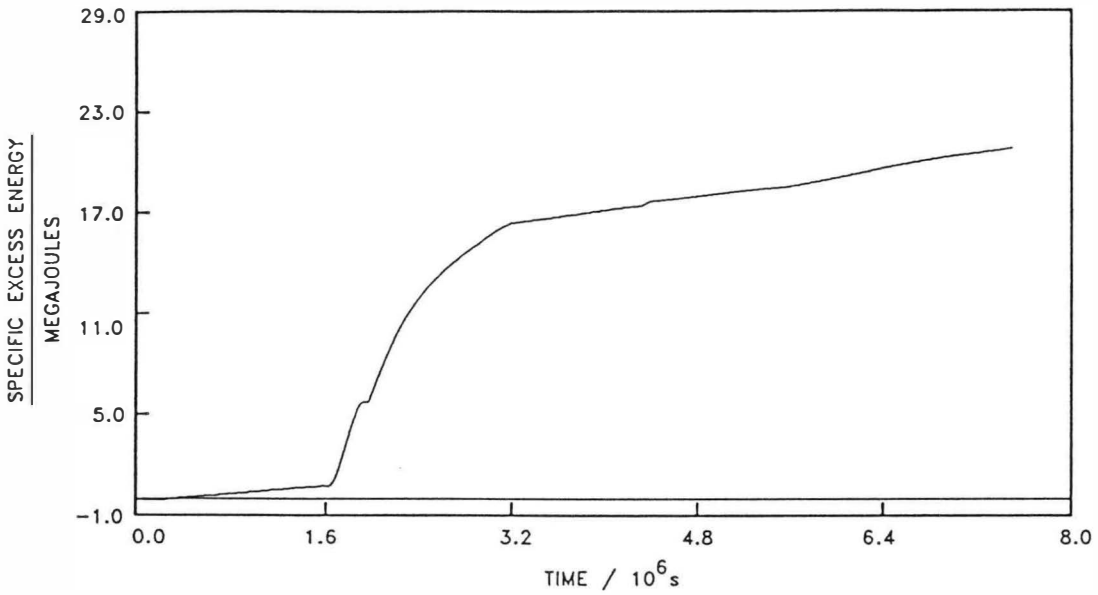

Fig 7C: The total specific excess enthalpy as a function of time for the experiment illustrated in Figs 7A and 7B.

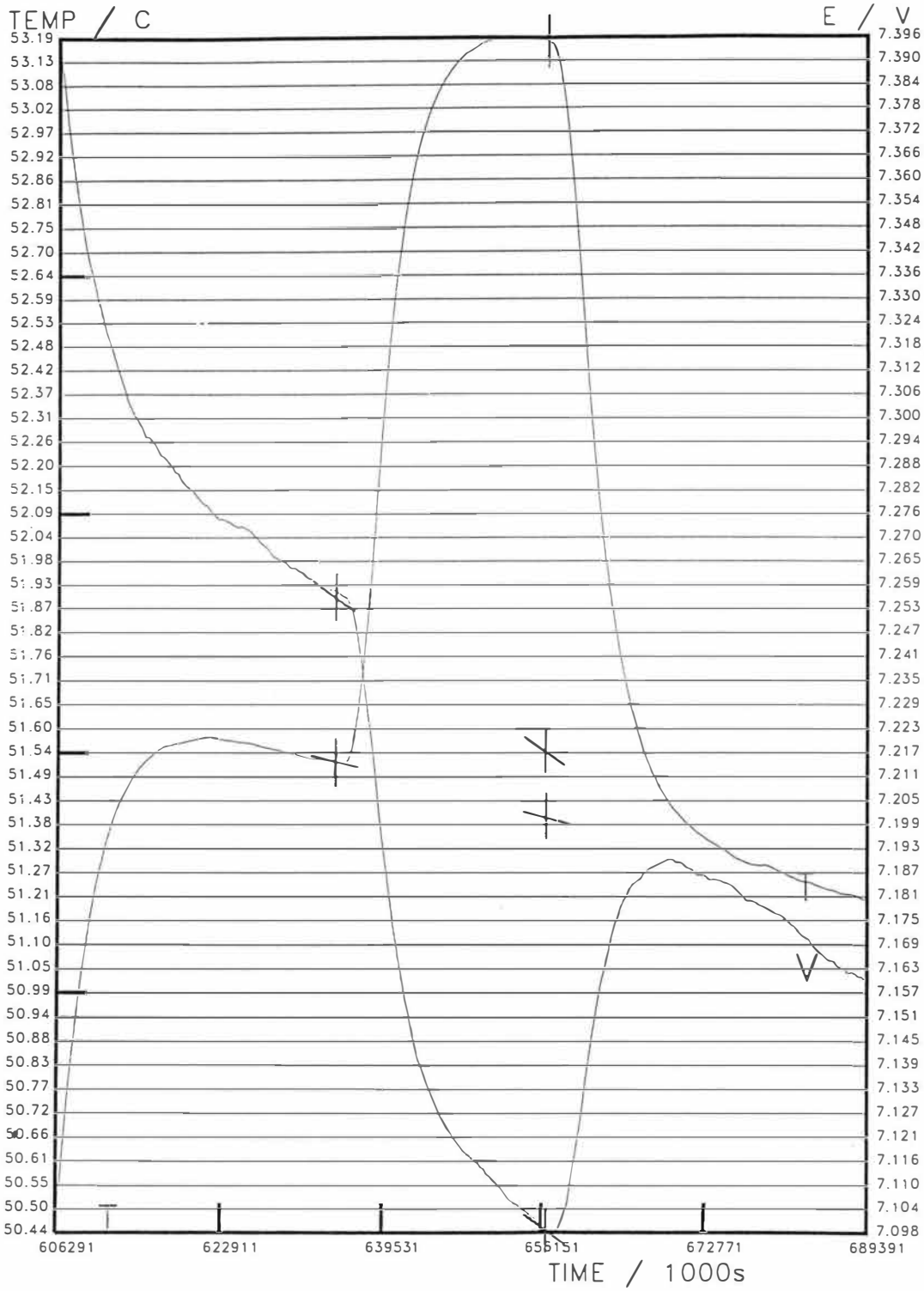

Fig 8A: Temperature-time and cell potential-time curves for the polarisation of a Pd90 Ag10 electrode in 0.1M LiOD in D_2O before the onset of "positive feedback". Electrode dimensions: 4mm diameter, 12.5mm length; cell current: 500mA.

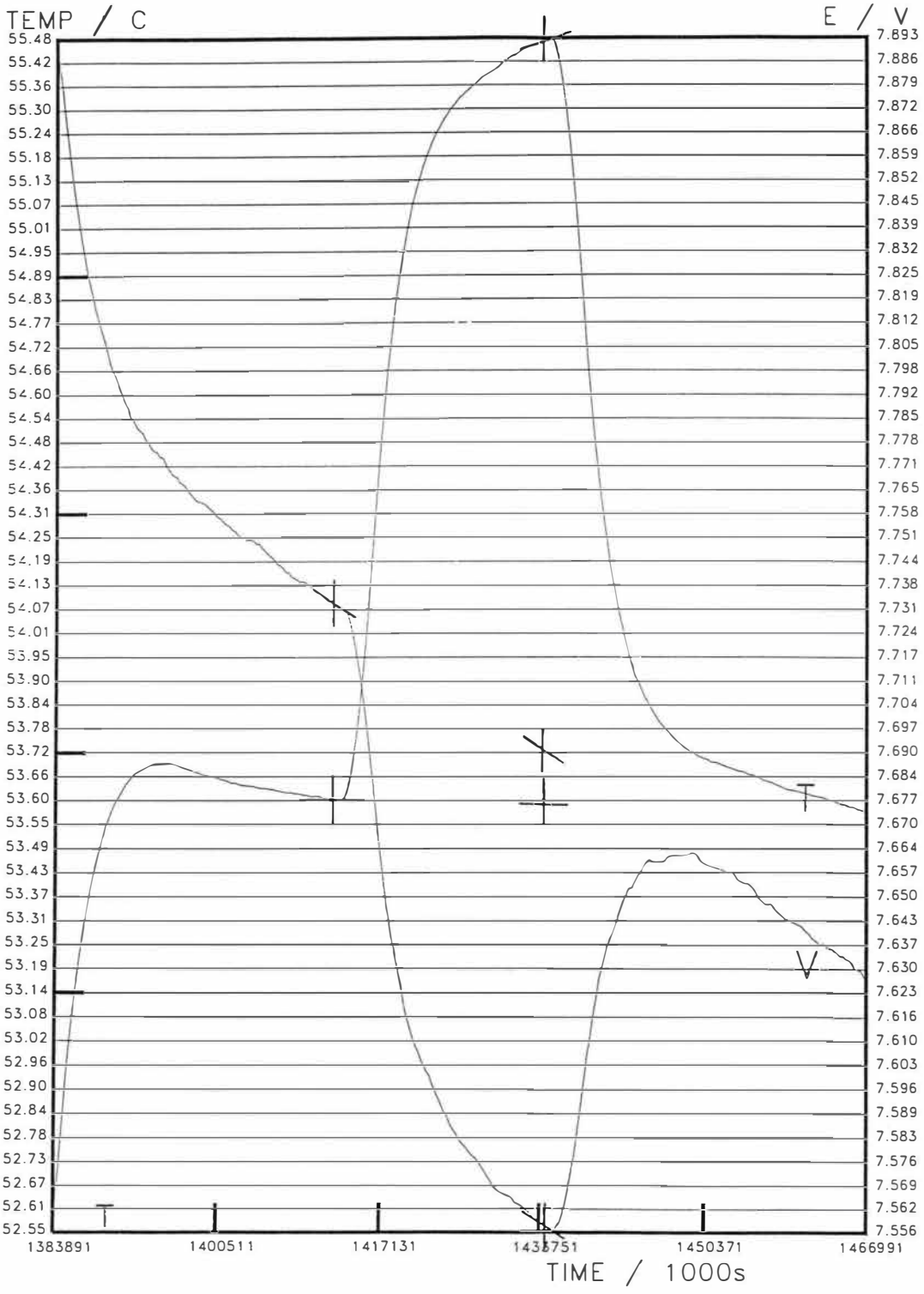

Fig 8B: The temperature-time and cell potential-time curves for the system illustrated in Fig 8A but during the stage of "positive feedback".

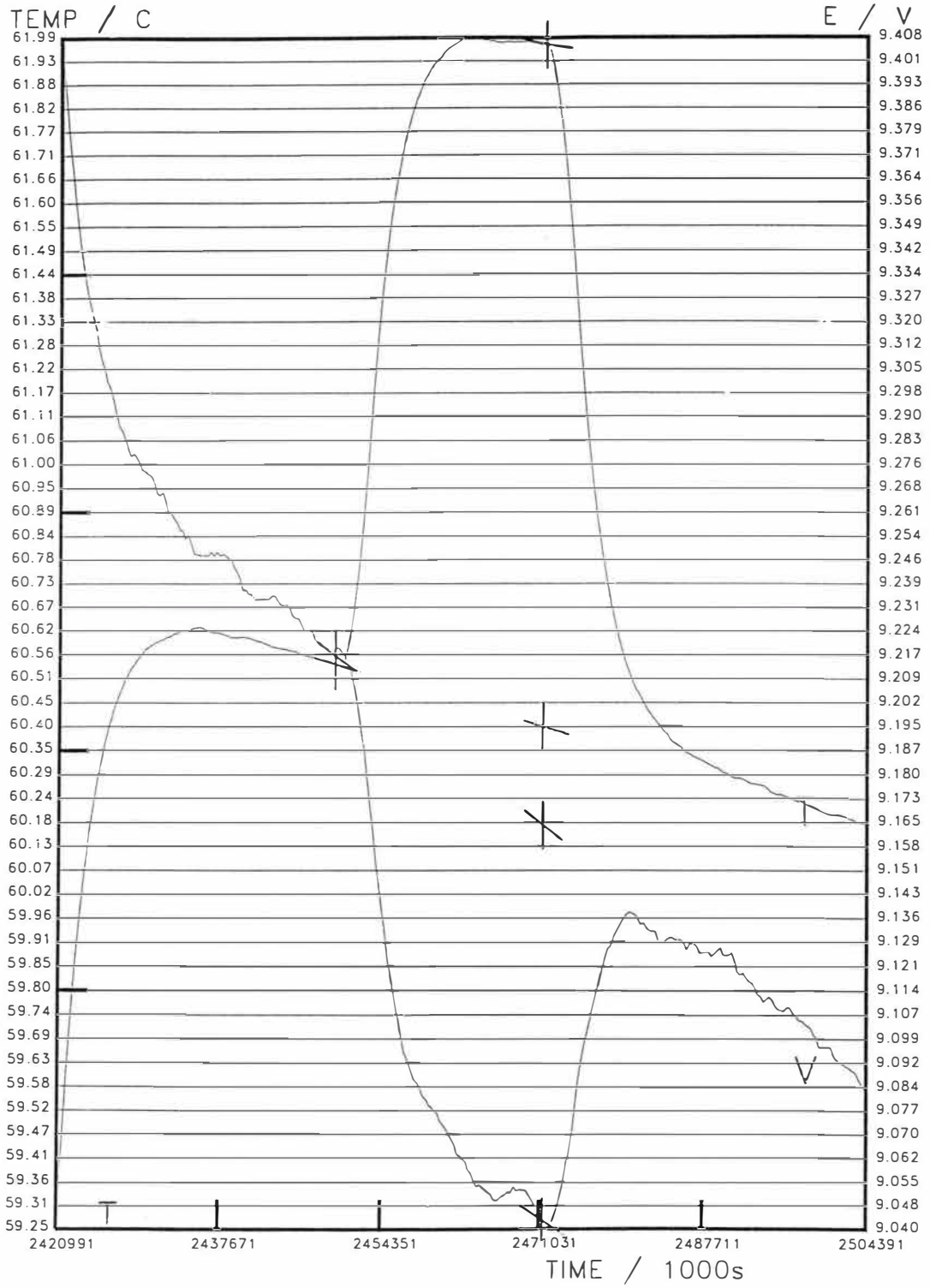

Fig 8C: The temperature-time and cell potential-time curves for the system illustrated in Figs 8A and 8B but after the completion of the stage of "positive feedback".

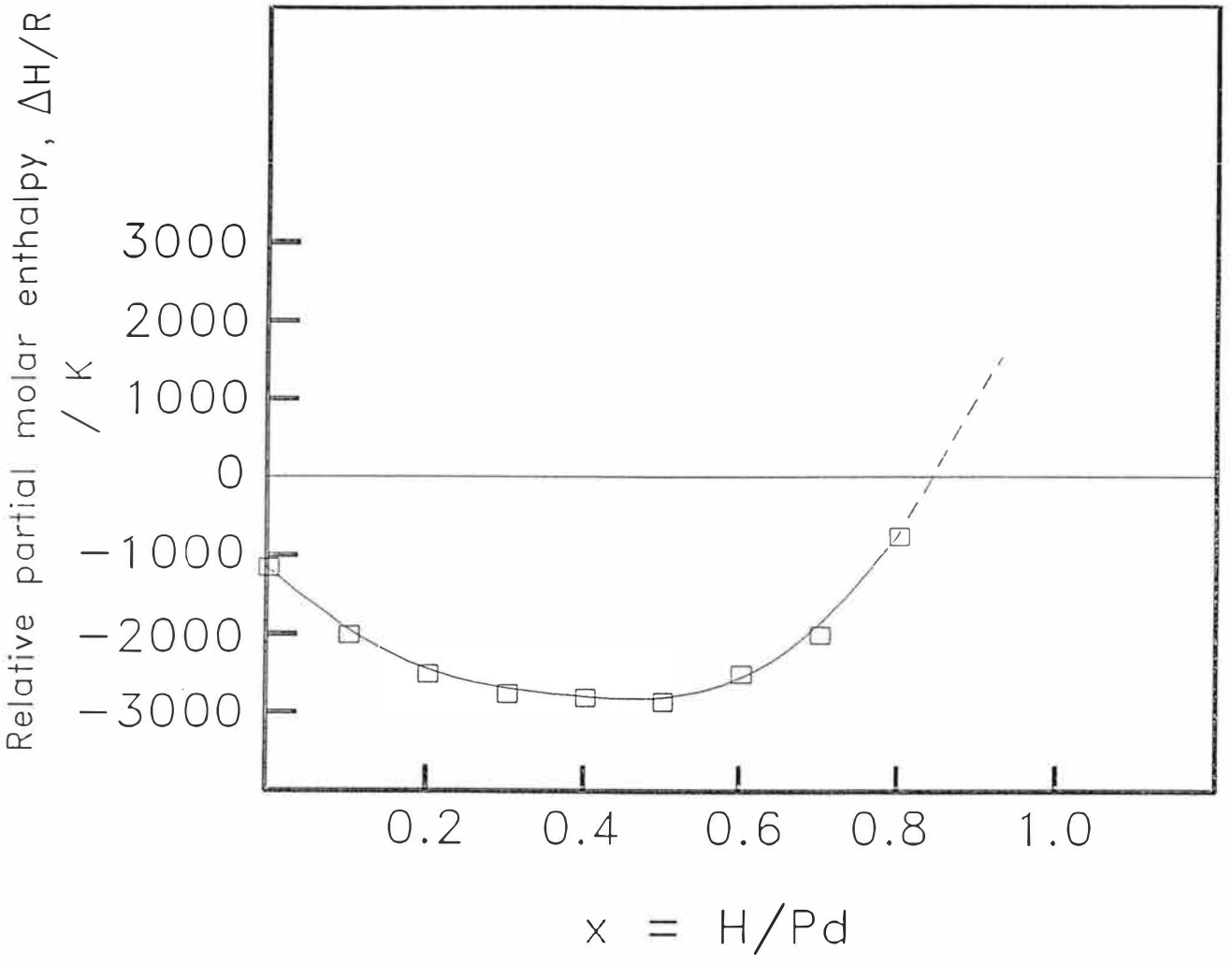

Fig 9: The variation of the relative partial molar enthalpy of absorption of hydrogen in palladium as a function of the charging ratio.

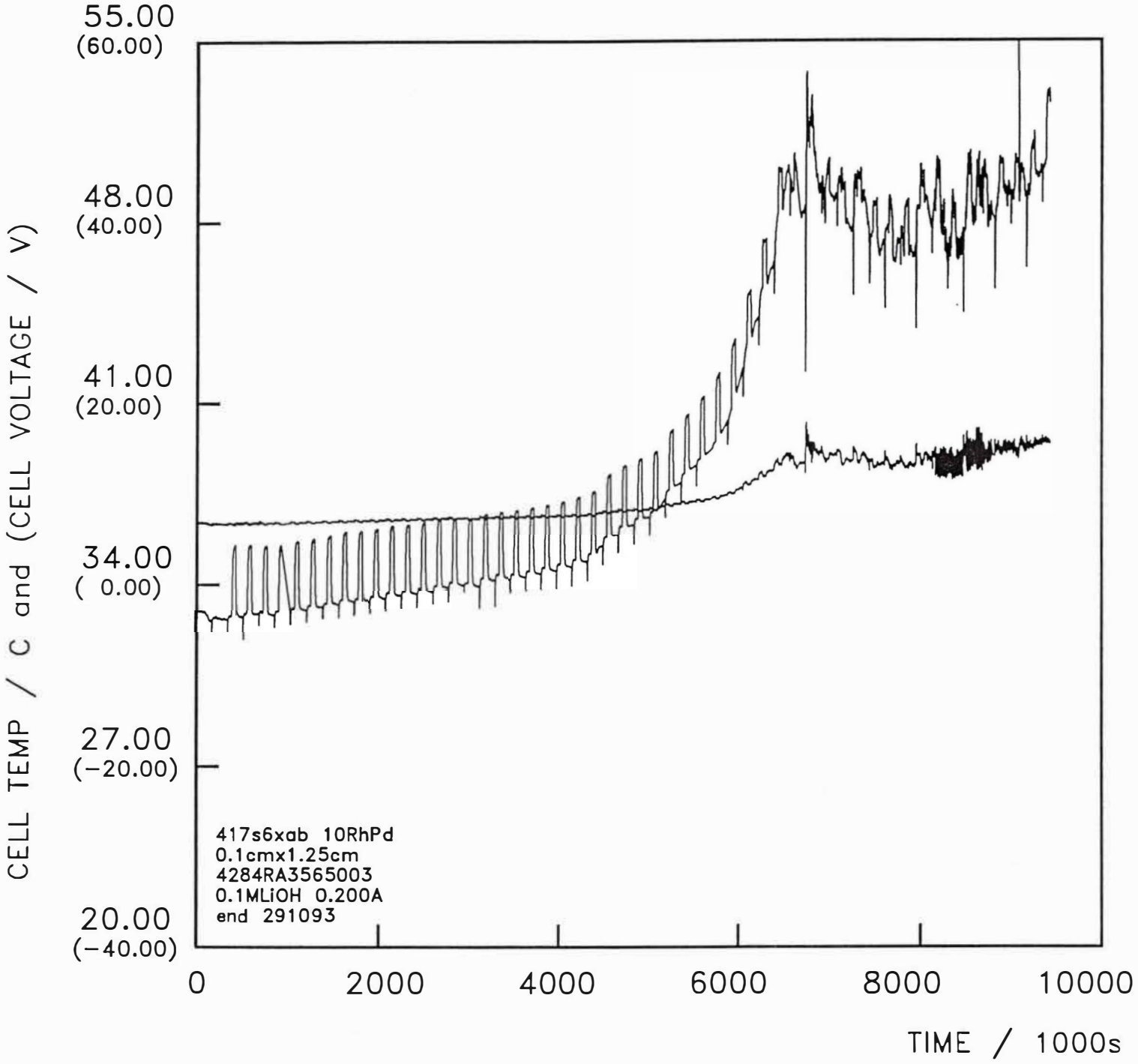

Fig 10A: Temperature-time and cell potential-time curves for the polarisation of a Pd90 Rh10 cathode in 0.1M LiOH in H_2O. Electrode dimensions: 1mm diameter, 12.5mm length; cell current: 200mA.

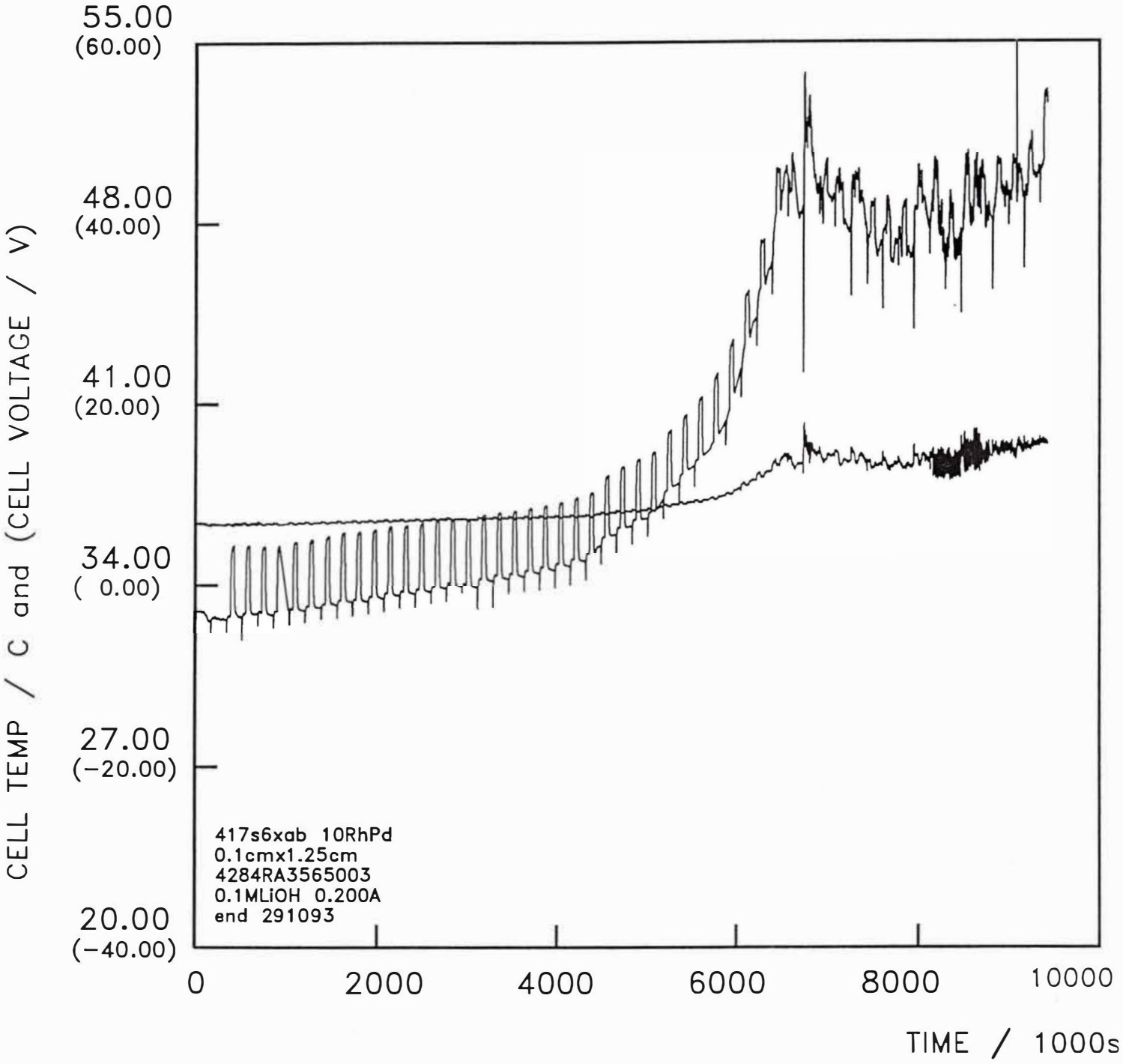

Fig 10B: Expanded section of Fig 10A.

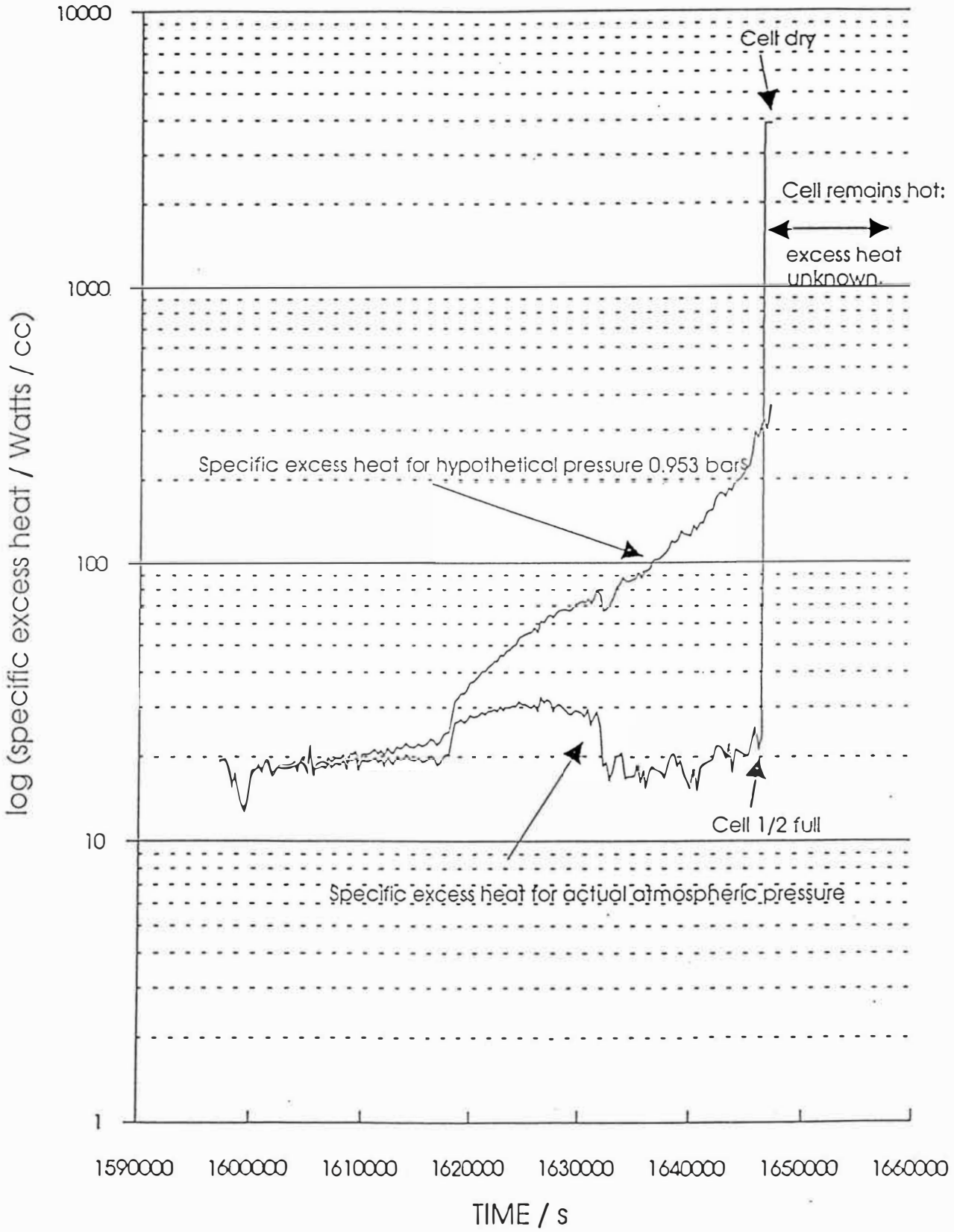

Fig 11: The variation of the specific excess enthalpy with time for the last stage of polarisation of the system illustrated in Figs 5A and 5B. The assumptions for the two plots shown are given in the text.